

Anion-specific surface valence-band states in heteropolar semiconductors: The case of GaP(110) and InP(110)

M. Sancrotti* and L. Duò

Dipartimento di Fisica, Politecnico di Milano, Piazza Leonardo da Vinci 32, 20133 Milano, Italy

L. Calliari

Istituto per la Ricerca Scientifica e Tecnologica, I-38050 Povo, Italy

F. Manghi

Dipartimento di Fisica, Università di Modena, Via Campi 213/A, 41100 Modena, Italy

R. Cosso and P. Weightman

IRC Surface Science, University of Liverpool, Oxford Street, L69 3BX Liverpool, United Kingdom

(Received 13 February 1992; revised manuscript received 17 July 1992)

The surface- and anion-specific valence-band states of heteropolar P containing III-V semiconductors [GaP(110) and InP(110)] have been determined by analysis of the Auger P $L_{2,3}VV$ line shape of the as-cleaved samples and the well-ordered epitaxial Sb-covered interfaces. The experimental spectra are analyzed in terms of slab-resolved partial density-of-states calculations performed for different surface structural models.

The coordination and spatial arrangement of atoms at solid surfaces give rise to a surface-specific electronic structure that can differ significantly from that of the bulk. A challenge for solid-state spectroscopies is to discriminate the surface electronic structure from that related to the bulk and a wide variety of approaches have been employed in attempts to characterize the electronic structure corresponding both to perfect truncation of the solid and as a result of surface relaxations and reconstructions. Although a large body of information is now available on surface core-levels shifts¹ on both metallic and semiconducting crystals, information on surface densities of states is currently restricted to transition and noble metals systems, notably the pioneering work on elemental Cu (Ref. 2) and Au (Ref. 3), where the dominance of the photoelectron cross section of the d states with respect to the sp contributions and the collection of electrons emitted at differently selected directions with respect to the surface normal made it possible to separate the $3d$ - and $5d$ -derived surface density of states (DOS), respectively, from the overall signal. For multiatomic compounds like the important III-V and II-VI semiconductors, where the valence DOS are of purely sp character, valence state photoemission spectroscopy is unable to distinguish either the chemical site or the orbital symmetry of the surface DOS. Consequently, whereas band mapping of surface states has been possible via photoemission,⁴ experimentally determined surface DOS have not yet been reported to III-V and II-VI compound semiconductors. In this connection, core-valence-valence (CVV) Auger spectroscopy has a unique potential for probing both the site-projected and orbital symmetry-projected density of (occupied) states in surface sensitive conditions.⁵ It gives, moreover, the opportunity to explore the

role of intrasite correlation effects for the two holes left behind the Auger transition.⁵

Here we demonstrate how the p -derived electronic structure of P atoms local to the surfaces of both GaP(110) and InP(110) can be determined by combining P $L_{2,3}VV$ Auger spectroscopy with epitaxial p -(1 \times 1) growth of one Sb monolayer (ML) on top of the as-cleaved surfaces. We exploit the well-established fact that the growth of Sb, which is isoelectronic with P, on top of III-V semiconductors,^{6,9} restores a bulklike environment for the topmost P atoms. This structural determination has been firstly obtained by dynamical low-energy electron diffraction analysis, whose interpretation benefited from total-energy minimization calculations.⁶ The basic idea underlying this work is that analysis of the difference spectrum obtained by subtracting the P $L_{2,3}VV$ line shape of the Sb-covered interface from the P $L_{2,3}VV$ profile of the as-cleaved semiconductors provides the self-convoluted distribution of valence-band states projected onto the P sites of the very surface layer. The experimental data are compared with single-particle theoretical calculations of the partial DOS relative to the reconstructed GaP(110) and InP(110) surfaces and the two p -(1 \times 1) Sb interfaces. Agreement and consistency are found between our experimental and theoretical results. Among heteropolar compounds III-V semiconductors are of special interest due to their technological applications as superlattices and quantum wells.¹⁰

n -type GaP and InP bars were cleaved along (110) planes in ultrahigh vacuum (base pressure $\approx 1 \times 10^{-10}$ mbar). Ultrapure Sb (99.9999%) was resistively evaporated from Ta crucibles at low evaporation rates (≈ 1 Å/min). During the overlayer growth the pressure was kept below 7×10^{-10} mbar. The thickness of deposited

Sb was measured with a quartz microbalance and checked *a posteriori* by measuring the peak-to-peak amplitude ratio of the P $L_{2,3}VV$ and Sb $M_{4,5}VV$ Auger lines. Here, 1 ML is defined in terms of the atomic surface density of GaP(110) (9.52×10^{14} at/cm²) and InP(110) (8.2×10^{14} at/cm²), corresponding to 2.91 and 2.5 Å, respectively. The Auger spectra were excited by a scanning resolved electron gun coaxial to a single-pass cylindrical mirror analyzer (CMA), which was used for the analysis of the electron energies. The intrinsic energy resolution of the CMA was 0.3%. The incident energy resolution of the CMA was 0.3%. The incident current density was set below 0.25 nA/ μm^2 to avoid charging effects. Measurements on different areas of the as-cleaved and interface systems provided reproducible results. During the experiments, the surface cleanliness was checked by monitoring the C and O KLL Auger signals, which were below typical Auger detection limits. Before and after each Sb evaporation sharp (1 \times 1) low-energy electron diffraction patterns were observed. Electron energy loss (EEL) spectra were acquired from the same spatial regions explored by Auger spectroscopy with the energy of the primary electron beam falling within the 120–150 eV kinetic-energy (KE) range to ensure the same surface sensitivity of the P $L_{2,3}VV$ electrons. Secondary electron spectra measured in the same KE range from thick Sb and In films confirmed the absence of Sb- and In-specific contributions to the P spectra studied.

Electron state bands and site- and orbital-projected partial DOS were calculated using a tight-binding description for a stack of 13 regularly spaced (110) slabs of GaP and InP. For the GaP/Sb and InP/Sb interfaces, Sb atoms were located at the two extreme (first and thirteenth) slabs. The tight-binding intra-atomic and extra-atomic parameters, determined via the total-energy minimization method, were taken from Ref. 6 along with the structural geometries of the reconstructed surfaces and epitaxial interfaces. We remark that the calculated DOS of the clean GaP(110) and InP(110) are in good agreement with measured valence-band photoemission data.¹¹

The P $L_{2,3}VV$ Auger transition, along with the similar and most widely explored Si $L_{2,3}VV$, is well known to exhibit bandlike behavior, i.e., it primarily reflects the self-folded valence DOS local to the core-hole excited site.⁵ This has been established in a wide variety of cases encompassing semiconducting and metallic compounds. It is also currently recognized that matrix-element effects modulate the relative intensities of the ll' two-hole final-state manifolds, the pp -character features being more intense than the sp - and ss -character structures.⁵ On this basis, experimental line shapes are usually compared with the so-called self-folded transition DOS $N(E) \cdot N(E)$, where $N(E) = N_p(E) + \alpha N_s(E)$ with $0 < \alpha < 1$ representing the weight with which the s symmetry versus p symmetry partial DOS are probed. In the case of the Si $L_{2,3}VV$ and P $L_{2,3}VV$ profiles $\alpha = 0.2 - 0.3$.¹² The theoretical Auger profiles are synthesized here by taking into account the relative population and splitting of the P $2p_{1/2}$ and P $2p_{3/2}$ initial-state holes. The branching ratio (1.85 for GaP and 2.09 for InP) and the spin-orbit split-

ting ($\Delta_{so} = 0.88$ eV for GaP and 0.87 eV for InP) have been taken from high-resolution photoemission data of the P $2p$ levels.^{13,14} For the surface layer, the experimental P $2p$ surface core-level shifts ($\Delta_{SCS} = 0.46$ eV for GaP and 0.29 eV for InP) have been used. All the experimental and calculated profiles herein shown are referenced to the valence-band maximum relative to the P $2p_{1/2}$ level binding energy (BE). In order to simulate the escape-depth effects occurring at the real P $L_{2,3}VV$ transition, the self-folded transition DOS of the different slabs were added using the weighted coefficients given by $\exp(-\lambda/z)$, where λ represents the empiric electron escape depth and z is the position of the various P sites normal to the surface. λ was chosen as 6.5 Å consistently with (i) the surface to bulk intensity ratio of the Ga $3d$ photoemission components excited with $h\nu = 145$ eV giving rise to photoelectrons KE's of about 120 eV, i.e., in the P $L_{2,3}VV$ Auger transition range;¹⁴ (ii) the value estimated via the empirical relation by Seah and Dench ($\lambda = 6$ Å);¹⁵ (iii) the extrapolation to high KE values of the escape-depth curve experimentally obtained by McLean and Ludeke for GaP(110) ($\lambda = 6.9$ Å).¹⁴ In the case of GaP the thus obtained attenuation coefficients for the first to seventh slabs are 1, 0.74, 0.55, 0.41, 0.30, 0.23, and 0.17. The error related to the finite number of included slabs is less than 4% of the total intensity. We remark that the final surface contribution is $\approx 30\%$ of the total intensity. Each CVV profile has been moreover Gaussian broadened ($\sigma_g = 1.2$ eV) to simulate lifetime effects. Our conclusion are not affected by small changes of

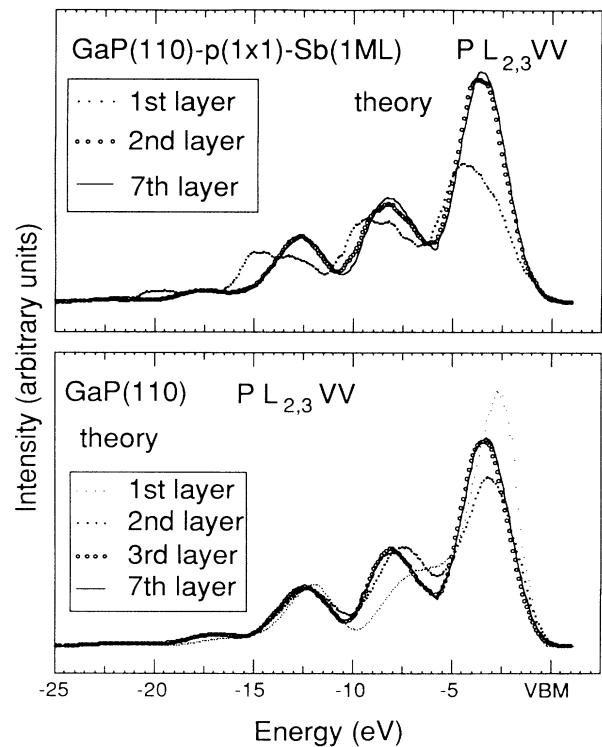


FIG. 1. P-specific self-folded transition density of states ($\alpha = 0.2$) for various atomic slabs of GaP considered in the relaxed (110) surface geometry (lower panel) and with the ordered Sb epilayer grown on top of it (upper panel).

$\approx 10\text{--}20\%$ in the values of λ , α , and σ .

In Fig. 1 are displayed the self-folded transition DOS ($\alpha=0.2$) relative to the first three slabs and to the seventh one of GaP with the surface assumed in the reconstructed configuration (lower panel) and with the ordered Sb epilayer (upper panel). The curves are shown as directly calculated with no weight coefficient. Analysis of the top panel of Fig. 1 and similar transition DOS establishes that the orbital symmetry and local coordination of surface and near-surface atoms of the uncovered substrates causes the CVV profiles of the first and second slabs to differ from each other and from the other planes whereas from the third slab on, no notable difference in shape can be identified. Furthermore (see upper panel of Fig. 1), Sb overlayers bring the topmost P atoms to behave similarly to the second P layer of the uncovered semiconductor. The electronic structure of the atoms underneath remain essentially unperturbed by the presence of the Sb epilayer. Similar conclusions can be drawn from analysis of the InP and InP/Sb systems.

Figure 2 shows a set of CVV profiles synthesized under different assumptions of the local surface environment, as follows: (a) the total CVV line shape of the uncovered semiconductors; (b) the same curve without the contribution of the first layer. Also shown is the self-folded p -symmetry partial DOS (second to seventh slabs) to give a visual aid to quantify the relative intensities of the differing $l'l'$ contributions; (c) the total CVV line shape (first to seventh slabs) for the two p - (1×1) Sb interfaces. All the curves have been normalized to their maximum height to facilitate direct comparison of the line shapes. Consideration of the depth-dependent attenuation in probing the various slabs is taken into account farther below. The results for the evolution of the slab-projected self-convoluted transition DOS as a function of the depth below the surface give rise to differences in the shape of the calculated CVV profiles depending on whether the first layer contribution is included in the line-shape synthesis. This may be seen in Fig. 2, where we note that the

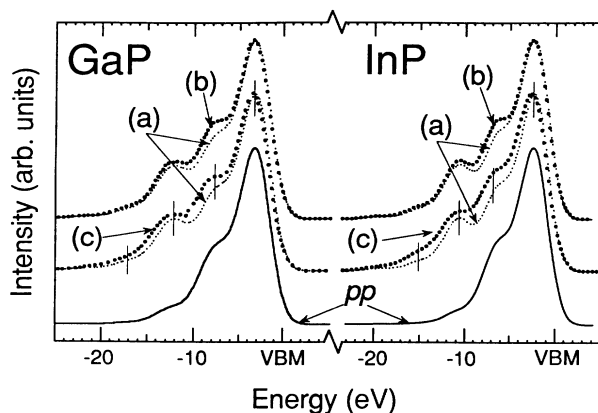


FIG. 2. P-specific synthesized CVV curved for different surface structural models of GaP(110), InP(110), and Sb-covered interfaces. (a) Total CVV line shape for the uncovered semiconductors; (b) as in (a) after having removed the contribution of the first layer; (c) total CVV profile for the III-V/Sb interfaces. The vertical bars identify the position of the main features in the profiles.

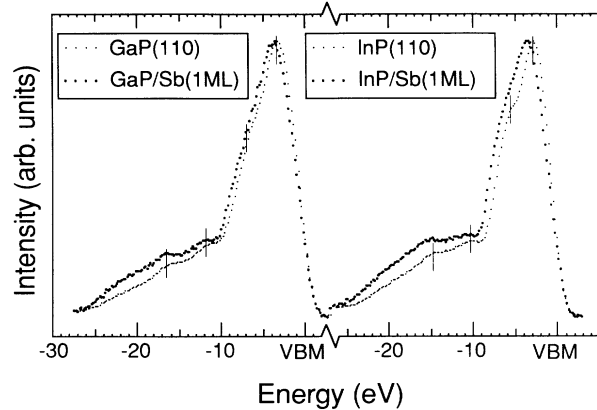


FIG. 3. Experimental P $L_{2,3}VV$ line shapes from the as-cleaved GaP(110) and InP(110) surfaces and the Sb-covered interfaces after background subtraction and energy-loss deconvolution. The vertical bars identify the position of the main features in the spectra.

exclusion of the first reconstructed layer from the CVV line shape [curves (b)] causes (i) the two bumps at about -8 and -13 eV to significantly increase in intensity relative to the maximum peak; (ii) the main peak, at about -3 eV, to shift about 0.5 eV to higher BE's; (iii) the tail at high BE's close to the valence-band maximum to change in the sense of a less steep slope. The same comments can be derived from the analysis of the curves (c).

In Fig. 3 in P $L_{2,3}VV$ line shapes measured from the as-cleaved GaP(110) and InP(110) surfaces (points) and from the p - (1×1) Sb interfaces (black circles) are displayed. The curves have been obtained after background subtraction (third-order polynomial) and deconvolution of the associated EEL profiles consistently with the procedure reported in Ref. 16. Changes in the background profile (e.g., integral versus second-order polynomial) do not significantly affect our general conclusions. The energy scales are referred to the valence-band maximum. This gives an excellent overlap of the tails at low BE's, as independently determined by the theory (Fig. 2). By looking at this figure we first note that the relative positions of the various features identified in the as-cleaved measurement are in good agreement with the calculation shown in Fig. 1, thereby confirming the validity of a bandlike description for the P $L_{2,3}VV$ Auger profile. Secondly, significant changes of the CVV line shape are observed when the epitaxial Sb overlayer is grown on top of the GaP(110) and InP(110) surfaces. These differences are in accordance with those predicted by the theory for the removal of the first layer contribution [curve (b) versus curve (a) in Fig. 2]. Thus, a careful line-shape analysis of the P $L_{2,3}VV$ Auger transition is able to highlight specific points characteristic of the surface structural model. This confirms *a posteriori* the expected role played by the Sb overlayer: to eliminate the semiconductor surface reconstruction and to restore a bulk-like condition for the topmost P atoms, both from the structural and electronic point of view. This conclusion makes meaningful the comparison of Fig. 4 where the reconstructed GaP(110) [InP(110)] self-folded transition DOS (open circles) of the surface layer is shown along

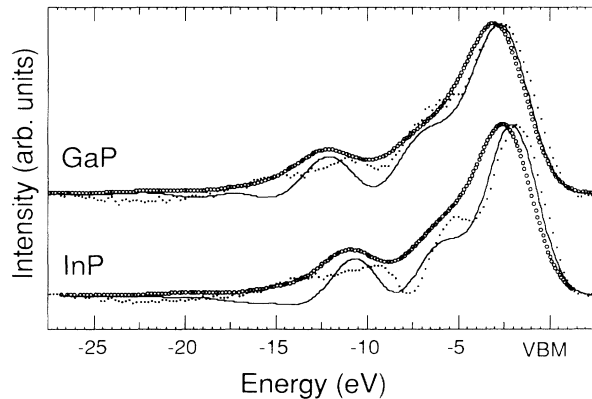


FIG. 4. Measured and calculated surface-specific P-related CVV line shapes for GaP(110) and InP(110). Open circles: self-folded transition DOS of the surface layer for the reconstructed GaP and InP geometries. Black dots: experimental difference spectrum. Solid line: theoretical difference spectrum. See the text for more details.

with the difference spectrum obtained by subtracting the Sb-covered Auger measurements from the as-cleaved line shapes (black dots). These two curves were considered in terms of their as-measured relative intensity thus explicitly taking into account the Sb-induced attenuation of the P $L_{2,3}VV$ signal for the III-V/Sb interfaces. Also shown is the difference curve (solid line) obtained by subtracting the CVV theoretical line shape of the Sb-covered interface—after intensity normalization so to simulate the overlayer-induced attenuation—from the total calculated CVV line shape of the clean surface. In the case of GaP, the two calculated profiles are very similar to each other and appear in excellent agreement with the experi-

mentally determined line shape, thereby confirming the experimental difference spectrum as the first direct measurement of the self-folded DOS local to surface anion atoms of a compound semiconductor. Also in the case of InP the qualitative agreement is good, although at a closer inspection, more pronounced dissimilarities appear between the two theoretical profiles—in particular the energy location of the main feature—and the agreement between experiment and theory improves as to the main peak position and relative intensity of the various features, when the effect of the Sb epilayer in the calculations is considered.

Before concluding, we note that even though final-state correlation effects can play some minor¹⁷ role in the measured P $L_{2,3}VV$ line shapes, our joint experimental and theoretical analysis is essentially based on difference curves (Figs. 3 and 4) and will be basically unaffected by such effects.

In conclusion, we have reported a joint theoretical and experimental study of the P $L_{2,3}VV$ Auger line shape of the GaP(110) and InP(110) surfaces. Use of an ordered Sb overlayer, restoring bulk like conditions for the topmost P atoms, has allowed us to discriminate the Auger profile relative to the reconstructed surfaces thereby probing a surface-specific site-projected DOS at the GaP(110) and InP(110) compound semiconductors.

We would like to thank C. Presilla and F. Sacchetti for kindly allowing access to their deconvolution code. This work was partially supported by the Science Programme of the European Community under a contract twinning the Departments of Physics of the Politecnico di Milano, University of Liverpool, and Trinity College of Dublin.

*Also at Laboratorio Tecnologie Avanzate Superfici e Catalisi, Istituto Nazionale Fisica della Materia, Padriciano 99, 34012 Trieste, Italy.

¹J. Spanjaard, C. Guillot, M. Desjonqueres, G. Treglia, and J. Lecante, *Surf. Sci. Rep.* **5**, (1985) 1; W. F. Egelhoff, *ibid.* **6**, 253 (1987).

²M. Metha and C. S. Fadley, *Phys. Rev. Lett.* **39**, 1569 (1977).

³P. H. Citrin, G. K. Wertheim, and Y. Baer, *Phys. Rev. Lett.* **41**, 1425 (1978).

⁴See, for example, *The Chemical Physics of Solid Surfaces and Heterogeneous Catalysis*, edited by D. A. King and D. P. Woodruff (Elsevier, New York, 1988), Vol. 5.

⁵R. Weibmann, and K. Müller, *Surf. Sci. Rep.* **105**, 251 (1981); P. Weightman, *Rep. Prog. Phys.* **45**, 753 (1982); D. E. Ramaker, *Appl. Surf. Sci.* **21**, 243 (1985).

⁶J. Carelli and A. Kahn, *Surf. Sci.* **116**, 280 (1982); C. Mailhot, C. B. Duke, and D. J. Chadi, *Phys. Rev. B* **31**, 2213 (1985).

⁷R. M. Feenstra and P. Mårtensson, *Phys. Rev. Lett.* **61**, 447 (1988).

⁸W. Drube and F. J. Himpsel, *Phys. Rev. B* **37**, 855 (1988).

⁹M. Hünerman, J. Geurts, and W. Richter, *Phys. Rev. Lett.* **66**, 640 (1991).

¹⁰See, for example, *Spectroscopy of Semiconductor Microstructures*, Vol. 206 of *Advanced Study Institute, Series B: Physics*, edited by G. Fasol, A. Fasolino, and P. Lugli (Plenum, New York, 1989).

¹¹L. Duo', M. Sancrotti, R. Cosso, S. D'Addato, A. Ruocco, S. Nannarone, D. Norman, and P. Weightman, *Phys. Rev. B* **42**, 3478 (1990).

¹²D. E. Ramaker, F. L. Hutson, N. H. Turner, and W. N. Mei, *Phys. Rev. B* **33**, 2574 (1986).

¹³T. Kendelewicz, K. Myano, R. Cao, J. C. Woicik, I. Lindau, and W. E. Spicer, *Surf. Sci.* **220**, L726 (1989).

¹⁴A. B. McLean and R. Ludeke, *Phys. Rev. B* **39**, 6223 (1989).

¹⁵M. P. Seah and D. Dench, *Surf. Interface Anal.* **1**, 2 (1979).

¹⁶V. Contini, C. Presilla, and F. Sacchetti, *Surf. Sci.* **210**, 520 (1989).

¹⁷P. O. Nilsson and S. P. Svensson, *Solid State Commun.* **79**, 191 (1991).